Ryanodine receptor/calcium release channel PKA phosphorylation: A critical mediator of heart failure progression

Xander H. T. Wehrens*†, Stephan E. Lehnart*†, Steven Reiken*†, John A. Vest*‡, Anetta Wronska*, and Andrew R. Marks*‡§

Departments of *Physiology and Cellular Biophysics and ‡Medicine, Clyde and Helen Wu Center for Molecular Cardiology, College of Physicians and Surgeons, Columbia University, New York, NY 10032

Defective regulation of the cardiac ryanodine receptor (RyR2)/calcium release channel, required for excitation-contraction coupling in the heart, has been linked to cardiac arrhythmias and heart failure. For example, diastolic calcium ''leak'' via RyR2 channels in the sarcoplasmic reticulum has been identified as an important factor contributing to impaired contractility in heart failure and ventricular arrhythmias that cause sudden cardiac death. In patients with heart failure, chronic activation of the ''fight or flight'' stress response leads to protein kinase A (PKA) hyperphosphorylation of RyR2 at Ser-2808. PKA phosphorylation of RyR2 Ser-2808 reduces the binding affinity of the channel-stabilizing subunit calstabin2, resulting in leaky RyR2 channels. We developed RyR2-S2808A mice to determine whether Ser-2808 is the functional PKA phosphorylation site on RyR2. Furthermore, mice in which the RyR2 channel cannot be PKA phosphorylated were relatively protected against the development of heart failure after myocardial infarction. Taken together, these data show that PKA phosphorylation of Ser-2808 on the RyR2 channel appears to be a critical mediator of progressive cardiac dysfunction after myocardial infarction.

calstabin2 | 12.6 kDa FK506-binding protein | myocardial infarction | sudden cardiac death

Heart failure (HF) is a complex systemic syndrome characterized by ventricular dysfunction resulting in shortness of breath and decreased exercise capacity (1). The most common cause of HF is ischemic coronary artery disease. Typically an initial impairment of cardiac function [e.g., loss of cardiac output due to myocardial infarction (MI)] leads to the activation of compensatory mechanisms in a long-term futile attempt to maintain contractility of the heart (2). For example, after myocardial damage, the sympathetic nervous system (SNS) and the renin angiotensin system become chronically activated. However, in the long term, chronic SNS activation contributes to progressive cardiac dysfunction (3, 4).

Under physiological conditions, activation of the evolutionarily conserved fight-or-flight response increases heart rate and cardiac contractility (5, 6). Indeed, in healthy hearts, SNS activation during exercise results in increased catecholamines that bind to and activate G protein-coupled β-adrenergic receptors on the plasma membrane that, in turn, activate adenylate cyclase. The resulting increase in cytosolic levels of cAMP activates the cAMP-dependent protein kinase A (PKA), which phosphorylates key Ca^{2+}-handling proteins, including the voltage-gated L-type Ca^{2+} channel (7), ryanodine receptor 2 (RyR2) (8), and phospholamban (PLB) (9). The net result is increased sarcoplasmic reticulum (SR) Ca^{2+} release via RyR2 and enhanced SR Ca^{2+} uptake by the SR Ca^{2+} pump (SERCA2a), resulting in larger intracellular Ca^{2+} transients. Increased Ca^{2+} transients significantly enhance contractility (inotropy) of the heart (6, 10).

Intracellular Ca^{2+} release via RyR2 is modulated by phosphorylation of the channel. The RyR2 channel comprises a large macromolecular signaling complex consisting of four RyR2 monomers, each binding one channel-stabilizing subunit calstabin2 [12.6-kDa FK506-binding protein (FKBP12.6)], as well as protein kinases (PKA and CaMKII), protein phosphatases (PP1 and PP2A), and a cAMP-specific type 4 phosphodiesterase (PDE4D3) (11) that are targeted to each RyR2 monomer via their respective anchoring proteins (12). Indeed, we have recently shown that RyR2 activity is regulated by local cAMP levels that are controlled by PDE4D3 in the RyR2 complex, providing an important negative-feedback mechanism to protect against continuous β-adrenergic receptor-dependent PKA phosphorylation of RyR2 (11). During HF, chronic activation of the fight-or-flight stress response results in down-regulation of PDE4D3 and PP1/PP2A in the RyR2 complex, contributing to a gain-of-function defect characterized by chronically increased PKA phosphorylation (hyperphosphorylation) of the RyR2 channel and progressive cardiac dysfunction (2, 13).

PKA hyperphosphorylation of RyR2 decreases the binding affinity of the channel-stabilizing subunit calstabin2, resulting in increased sensitivity of the channel to Ca^{2+}-dependent activation (8). Recent studies have confirmed that increased PKA phosphorylation of RyR2 results in a diastolic SR Ca^{2+} leak in cardiomyocytes that contributes to chronically reduced SR Ca^{2+} content and diminished contractility in HF (8, 14). However, other investigators using different model systems have challenged some aspects of these findings (15, 16). In addition, decreased SR Ca^{2+} uptake by SERCA2a, and increased Ca^{2+} extrusion via the Na^+/Ca^{2+}-exchanger also contribute to decreased SR Ca^{2+} loading and decreased cardiac contractility (17, 18).

In the present study, we genetically ablated the RyR2-S2808A PKA phosphorylation site in the murine RyR2. RyR2-S2808A channels from mouse hearts resembled wild-type (WT) RyR2 under resting conditions but could not be PKA phosphorylated during activation of the β-adrenergic signaling pathway *in vivo*, indicating that Ser-2808 is the functional PKA site in RyR2. Importantly, when subjected to myocardial infarction, RyR2-S2808A mice exhibited significantly improved cardiac function compared with WT mice. Thus, PKA phosphorylation of RyR2 at Ser-2808, which reduces calstabin2 binding to RyR2 and
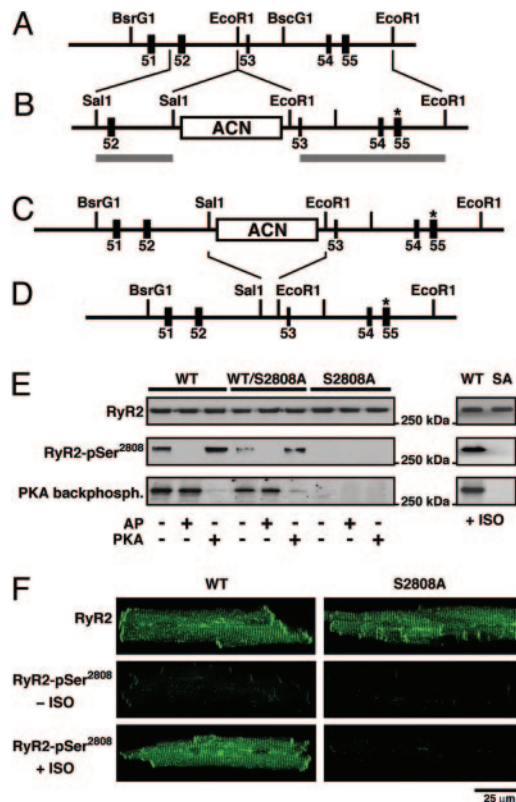

Fig. 1. Lack of PKA phosphorylation of RyR2 in RyR2-S2808A mice. (*A*) The wild-type locus of the murine *RyR2* gene containing exons 51–55. (*B*) The targeting construct containing 2.4- and 5.4-kb homologous regions (horizontal gray lines). The S2808A mutation (∗) is engineered in exon 55. (*C*) The homologous recombinant mutant allele containing the RyR2-S2808A mutation and the ACN selection marker cassette. (*D*) Final RyR2-S2808A allele after excision of the ACN selection marker. (*E*) Representative Western blot analysis by using a phospho-specific antibody recognizing PKA-phosphorylated Ser-2808 on RyR2 and PKA kinasing reaction both demonstrate that RyR2-S2808A channels from mice cannot be PKA-phosphorylated. RyR2 immunoprecipitated from cardiac lysates from WT, heterozygous WT/RyR2-S2808A, and RyR2-S2808A mice were treated with alkaline phosphatase (AP) or protein kinase A (PKA), respectively (*Left*). In addition, WT and RyR2-S2808A (SA) mice were injected with isoproterenol (*Right*). (*F*) Representative confocal images of isolated cardiomyocytes immunolabeled with antibodies detecting the RyR2 protein (*Top*) or the PKA-phosphorylated form of RyR2 at Ser^{2808} (*Center* and *Bottom*). *Center* and *Bottom* represent isolated cardiomyocytes untreated or treated with isoproterenol, respectively.

causes leaky RyR2 channels, is an important determinant of maladaptive remodeling and progressive cardiac dysfunction after myocardial infarction.

Results

RyR2 Cannot Be PKA Phosphorylated in RyR2-S2808A Mice. RyR2-S2808A mice generated by homologous recombination, resulted in the substitution of an alanine residue for Ser-2808 in RyR2 (Fig. 1 *A–D*). RyR2-S2808A mice are viable and fertile and were born at the expected Mendelian frequencies: WT/WT ($n = 61$, 26%), WT/RyR2-S2808A ($n = 111$, 47%), RyR2-S2808A/RyR2-S2808A ($n = 62$, 27%). Hearts of RyR2-S2808A mice were structurally normal based on longitudinal echocardiographic followup (at 3, 6, 9, and 12 months) and histology (at 6 and 12 months) (Fig. 7, which is published as supporting information on the PNAS web site).

To test whether RyR2 from RyR2-S2808A mice could be phosphorylated by PKA, RyR2 immunoprecipitated from cardiac lysates were subjected to a kinasing reaction by using PKA.
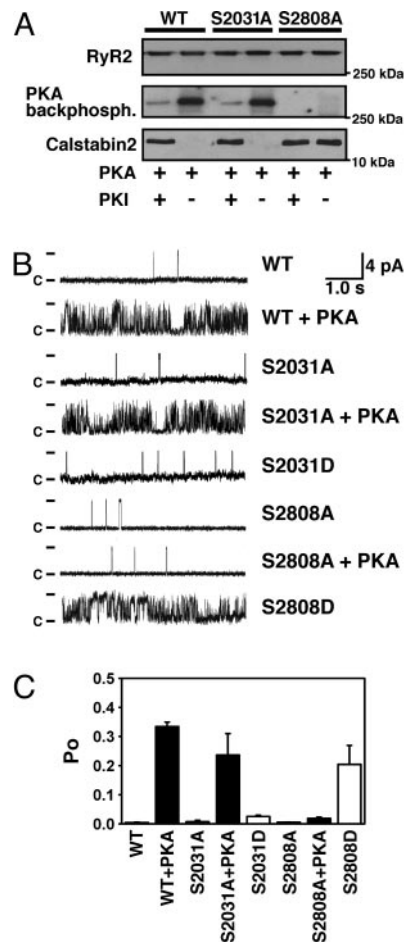

Fig. 2. PKA phosphorylation of Ser-2808 but not Ser-2031 modulates RyR2 single-channel activity. (*A*) Representative WT and mutant recombinant human RyR2 channels, coexpressed with calstabin2 (FKBP12.6), were PKA-phosphorylated in the presence or absence of the PKA-inhibitor PKI$_{5–24}$. Alanine substitution of Ser-2808, but not Ser-2031, prevents PKA phosphorylation of RyR2. Moreover, PKA phosphorylation of WT and RyR2-S2031A channel reduced the binding affinity of the RyR2 subunit calstabin2, whereas calstabin2 did not dissociate from RyR2-S2808A channels treated with PKA. (*B*) Single-channel recordings of RyR2-WT and mutant RyR2. PKA phosphorylation of RyR2-WT and RyR2-S2031A channels increased Po at low-cytosolic Ca^{2+} concentrations (150 nM), whereas the mutant RyR2-S2808A channels did not exhibit PKA phosphorylation-induced increase in Po. The Asp substitution of Ser-2031 functionally mimicked PKA phosphorylation of this residue but did not cause an increase in Po of the RyR2-S2031D channels. In contrast, RyR2-S2808D channels mimicked constitutively PKA-phosphorylated RyR2-WT channels, confirming that Ser-2808 is the only functional PKA site on RyR2. (*C*) Summary values of Po of single-channel recordings described in *B* ($n = 4$–9 channels in each group).

Samples were pretreated with alkaline phosphatase (AP) to maximally dephosphorylate PKA sites before PKA phosphorylation. In WT mice, PKA phosphorylation of Ser-2808 on RyR2 was readily detected by using a phospho-epitope-specific antibody (RyR2-pSer^{2808}; Fig. 1*E*). These results were confirmed by using a PKA backphosphorylation assay: (*i*) phosphorylation of WT RyR2 in the presence of [γ-^{32}P]-ATP resulted in a strong band and WT RyR2 was only weakly phosphorylated under baseline conditions, (*ii*) no additional [γ-^{32}P]-ATP could be incorporated into PKA phosphorylated RyR2, and (*iii*) no [γ-^{32}P]-ATP could be incorporated into RyR2-S2808A channels under any of the aforementioned conditions (Fig. 1*E*). Moreover, RyR2 channels from heterozygous WT/RyR2-S2808A mice could be PKA-phosphorylated, resulting in a reduced signal
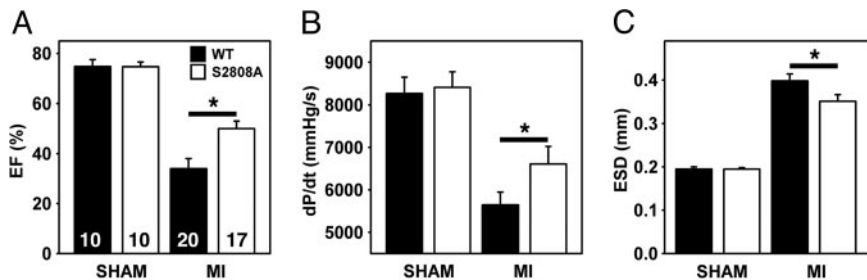
Fig. 3. Increased cardiac contractility in RyR2-S2808A mice 4 weeks after MI. (*A*) Quantification of M-mode echocardiograms showing increased ejection fraction (EF) in RyR2-S2808A mice compared with WT. *, $P < 0.05$. Number of mice as indicated. (*B*) Pressure-volume loops showing increased cardiac contractility in RyR2-S2808A mice compared with WT. dP/dt, maximum slope of the derivative of change in systolic pressure over time. (*C*) Echocardiographic quantification of the end-systolic diameter (ESD) showing reduced cardiac remodeling in RyR2-S2808A mice compared with WT.

compared to WT RyR2 channels, consistent with the presence of heterotetrameric RyR2 channels that contain both WT and RyR2-S2808A protomers.

To show that the RyR2-S2808A mutation prevented PKA phosphorylation of RyR2 *in vivo*, we infused 5 ng·kg^{-1}·min^{-1} isoproterenol for 2 min into the left jugular vein of RyR2-S2808A and WT mice after which the heart was flash-frozen in liquid nitrogen. Isoproterenol, a β-adrenergic receptor agonist, activates PKA and previously has been shown to cause PKA phosphorylation of RyR2 (19). In contrast to RyR2 immuno-precipitated from WT mice, RyR2-S2808A channels were not PKA phosphorylated after *in vivo* isoproterenol treatment (Fig. 1*E Right*). We also tested whether exposure to isoproterenol would increase PKA phosphorylation of RyR2 in cardiomyocytes isolated from WT and RyR2-S2808A mice (Fig. 1*F*). Using anti-RyR2 antibodies, immunolabeling corresponding with the Z-lines was observed in both WT and RyR2-S2808A cardiomyocytes. In cardiomyocytes isolated from WT mice, activation of the β-adrenergic receptor signaling pathway by isoproterenol caused increased PKA phosphorylation of RyR2-Ser-2808. However, no increase in PKA phosphorylation was detected in cardiomyocytes isolated from RyR2-S2808A mice. Taken together, these data demonstrate that the single mutation of Ser-2808 to an Ala in the native murine RyR2 is sufficient to eliminate all detectable PKA phosphorylation of RyR2 both *in vitro* and *in vivo*.

Ser-2808 Is the Dominant PKA Site on RyR2. Recently, Xiao *et al.* (15) proposed that Ser-2030 represents an additional PKA phosphorylation site in the murine RyR2 based on phosphopeptide mapping and site-directed mutagenesis. This finding is at odds with previous studies including phosphopeptide mapping (20), site-directed mutagenesis (8, 19, 21), and data in the present study obtained by using the RyR2-S2808A mice (Fig. 1). Nevertheless, we sought to directly test whether there is any evidence in support of RyR2-Ser-2030 as an additional PKA site in RyR2. Accordingly, we generated serine-to-alanine mutations of Ser-2031 (corresponding to Ser-2030 in mice) in the recombinant human RyR2 channel. RyR2-WT channels were readily phosphorylated by PKA, and PKA phosphorylation of WT RyR2 was inhibited by the addition of the specific PKA-inhibitor PKI$_{5–24}$ (Fig. 2*A*). RyR2-S2808A channels could not be PKA phosphorylated, as described in ref. 19. In contrast, we observed a robust PKA phosphorylation signal in RyR2-S2030A channels that was not significantly different from RyR2-WT channels, suggesting that Ser-2030 on RyR2 is not a PKA phosphorylation site.

PKA phosphorylation of the RyR2-WT channel reduces the binding affinity of the RyR2 channel subunit calstabin2 (FKBP12.6) (8, 21). Calstabin2 binding to RyR2-S2808A mutant channels did not decrease upon treatment with PKA (because the RyR2-S2808A channels cannot be PKA-phosphorylated),

whereas calstabin2 binding to PKA phosphorylated RyR2-WT and RyR2-S2030A channels was significantly decreased (Fig. 2*A*). Taken together, these data further indicate that Ser-2808, but not Ser-2030, is the PKA phosphorylation site on RyR2.

We examined the single-channel function of WT and mutant RyR2 in the presence of low-cytosolic Ca^{2+} (150 nM) by using Ca^{2+} as a charge carrier. The open probability (Po) of RyR2-WT channels at these Ca^{2+} concentrations (which correspond to the level of cytosolic Ca^{2+} during diastole in the heart) was low, as previously described (Fig. 2 *B* and *C*). The Po of WT channels increased after PKA phosphorylation (Fig. 2 *B* and *C*) because PKA phosphorylation and dissociation of calstabin2 (Fig. 2*A*) increase the sensitivity of the RyR2 channel to Ca^{2+}-induced activation. Similar to RyR2-WT channels, the Po of RyR2-S2031A channels also increased after PKA phosphorylation (Fig. 2 *B* and *C*), providing further evidence that Ser-2031 is not a functionally important PKA site on the RyR2 channel. Moreover, the single-channel properties of RyR2-S2031D channels (which mimics constitutive PKA phosphorylation at Ser-2031) were not significantly different from non-PKA phosphorylated RyR2. However, in contrast, as noted above, PKA-phosphorylated RyR2-WT channels and RyR2-S2808D channels both exhibited marked changes in single-channel function, characterized primarily by a significant increase in open probability. These findings confirm that Ser-2031 is not responsible for the effects of PKA phosphorylation on native RyR2 channel function. In contrast, the RyR2-S2808A mutation prevented the changes in single channel function caused by PKA phosphorylation of RyR2. Moreover, the single-channel properties of mutant RyR2-S2808D channels (that mimic constitutive PKA phosphorylation at Ser-2808) were not significantly different from PKA-phosphorylated RyR2-WT channels (Fig. 2 *B* and *C*). Taken together, these data support the previously reported findings that Ser-2808 is the only PKA site on RyR2 and mediates RyR2 channel activation by PKA phosphorylation.

Prevention of PKA Phosphorylation of RyR2 Improves Cardiac Function After MI. To determine the functional importance of PKA phosphorylation of RyR2 during the development of ischemic HF, we subjected WT and RyR2-S2808A mice to MI by ligation of the left anterior descending coronary artery (14), a procedure that results in progressive cardiac dysfunction leading to HF. Echocardiography at 28 days after MI demonstrated a significantly higher ejection fraction in RyR2-S2808A mice compared with WT mice (Fig. 3*A*), indicating that prevention of RyR2 PKA phosphorylation inhibits the progression of cardiac dysfunction after MI. Improved cardiac function in RyR2-S2808A mice was also evidenced by additional echocardiographic measurements, including increased fractional shortening, stroke volume, and smaller end-diastolic diameters (Table 1). Cardiac catheterization at 28 days after MI revealed reduced end-systolic volumes

Table 1. Cardiac function in WT and RyR2-S2808A mice at 4 weeks after MI

	WT (20)	S2808A (17)
Age, months	5.0 ± 0.3	4.8 ± 0.3
Body weight, g	24.99 ± 0.67	25.11 ± 0.89
Infarct size, %	36.50 ± 3.10	36.05 ± 3.27
HW/BW ratio	7.65 ± 0.39	8.32 ± 0.43
Echocardiography		
Ejection fraction, %	33.76 ± 3.67	50.43 ± 3.29*
Fractional shortening, %	14.86 ± 1.93	22.73 ± 2.00**
Stroke volume, μl	87.6 ± 0.74	112.6 ± 0.75*
LVPW, mm	0.84 ± 0.01	0.78 ± 0.02**
EDD, mm	5.21 ± 0.13	4.70 ± 0.13*
ESD, mm	3.98 ± 0.16	3.51 ± 0.15*
Cardiac catheterization		
dP/dt, mmHg/s	5,641 ± 304	6,810 ± 397*
−dP/dt, mmHg/s	−4,804 ± 275	−5,917 ± 412*
MAP	75.85 ± 2.30	80.30 ± 3.91

Analysis of *in vivo* cardiac size and function by echocardiography and cardiac catheterization in wild-type and RyR2-S2808A mice. Number in parentheses represents number of mice. LVPW, left ventricular posterior wall thickness; EDD, end-diastolic diameter; ESD, end-systolic diameter; dP/dt, slope of the maximal derivative of change in pressure over time; −dP/dt, slope of the maximal negative derivative of change in pressure over time; MAP, mean arterial blood pressure. *, $P < 0.05$; **, $P < 0.01$.

and increased cardiac contractility (dP/dt_{max}) in RyR2-S2808A mice (6,810 ± 397 mmHg/s; 1 mmHg = 133 Pa) compared with WT (5,641 ± 304 mmHg/s; $P < 0.05$, $n = 17$–20, see Fig. 3 *B* and *C*). The increase in cardiac contractility could not be explained by differences in heart rate or blood pressure comparing WT and RyR2-S2808A mice (Table 1). These data indicate that prevention of PKA phosphorylation of RyR2 after MI was also associated with a significant inhibition of the deleterious remodeling of the heart (e.g., chamber dilatation associated with decreased cardiac function) that is typically observed after MI.

RyR2 channels isolated from WT mice 28 days after MI were PKA hyperphosphorylated compared to sham-operated WT control mice (Fig. 4 *A* and *B*), in agreement with previous studies in humans and animal models (8, 14, 22–25). In contrast, RyR2 were not PKA hyperphosphorylated in RyR2-S2808A mice after MI (Fig. 4*A*). The findings based on the use of a RyR2-pSer[2808] phospho-epitope specific antibody were confirmed by using a PKA backphosphorylation assay, which detected no incorporation of [γ-^{32}P]-ATP into RyR2-S2808A channels in both sham-operated and post-MI mice (data not shown). PKA hyperphosphorylation of RyR2 in WT mice after MI resulted in decreased calstabin2 binding to RyR2, whereas calstabin2 binding to RyR2 was unaltered in RyR2-S2808A mice after MI (Fig. 4). CaMKII phosphorylation of RyR2-Ser-2814 was not altered after MI in WT or RyR2-S2808A mice, suggesting that CaMKII phosphorylation of RyR2 does not play an important role in the pathogenesis of ischemic heart failure after MI (Fig. 4). Thus, our findings indicate that genetic ablation of PKA-hyperphosphorylation after MI inhibits the progression of cardiac dysfunction.

Because defective SR Ca^{2+} uptake has also been correlated with depressed cardiac function in HF (17, 26), we examined SERCA2a and PLB protein levels and PLB phosphorylation in WT and RyR2-S2808A mice. After MI, SERCA2a expression was slightly decreased in both WT and RyR2-S2808A mice [$P =$ not significant (N.S.), $n = 8$–10, Fig. 4*A*]. PLB levels in the heart were also slightly lower in WT mice and RyR2-S2808A mice after MI ($P =$ N.S., $n = 8$–10, Fig. 4*A*). Although there were no significant alterations in CaMKII phosphorylation levels of PLB-Thr-17, PLB-Ser-16 was significantly hypophosphorylated in both WT and RyR2-S2808A mice after MI (Fig. 4 *A* and *B*).
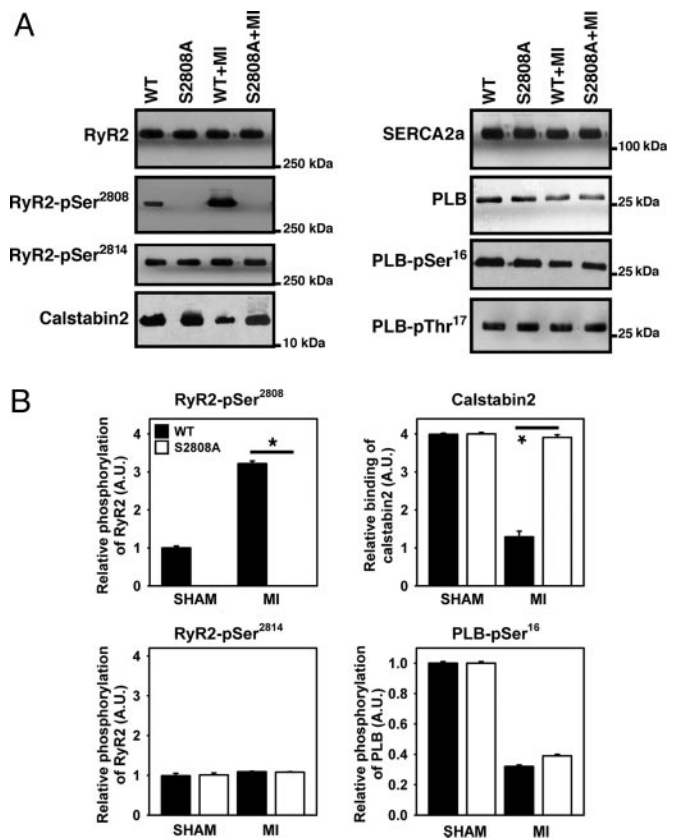

Fig. 4. MI does not cause PKA hyperphosphorylation of RyR2 and calstabin2 dissociation in RyR2-S2808A mice. Equivalent amounts of RyR2 were immunoprecipitated from cardiac lysates by using an anti-RyR2 antibody. Representative immunoblots (*A*) and bar graphs (*B*) show the amount of PKA and CaMKII phosphorylation of RyR2 as well as the amount of calstabin2 associated with RyR2 (*Left*). In contrast to WT mice, RyR2-S2808A mice did not develop PKA hyperphosphorylation of RyR2 after MI. A slight reduction in SERCA2a and PLB expression was observed in both WT and S2808A mice, whereas PLB was hypophosphorylated at Ser-16 in both infarcted WT and S2808A mice ($n = 9$, $P =$ N.S.).

Decreased RyR2 Channel Leak in RyR2-S2808A Mice After MI. We examined RyR2 single channels in the presence of low-cytosolic Ca^{2+} (150 nM) by using Ca^{2+} as a charge carrier. This Ca^{2+} concentration corresponds to cytosolic [Ca^{2+}] in the heart muscle during diastole, when the RyR2 channels in normal nonfailing hearts are closed to prevent a diastolic SR Ca^{2+} leak (27). Under the same conditions, the Po of RyR2 channels from WT mice subjected to MI was significantly higher compared with those of cardiac RyR2 channels from RyR2-S2808A mice (Fig. 5). The average Po was 0.498 ± 0.098 ($n = 7$) for WT mice with HF and 0.101 ± 0.038 ($n = 5$) for RyR2-S2808A mice subjected to MI ($P < 0.05$). Consistent with previous studies in RyR2 channels depleted of calstabin2, we observed subconductance states in cardiac RyR2 from WT mice after MI (14). In contrast, RyR2 channels from RyR2-S2808A mice subjected to MI displayed full channel openings and long-lasting closed states (Fig. 5*A*). These observations suggest that prevention of RyR2 PKA hyperphosphorylation, which is associated with preserved calstabin2 levels in the channel complex, is responsible for normal RyR2 channel properties and improved cardiac function in RyR2-S2808A mice after MI.

Discussion

The present study shows that prevention of PKA hyperphosphorylation of the cardiac RyR2 SR Ca^{2+} release channel inhibits
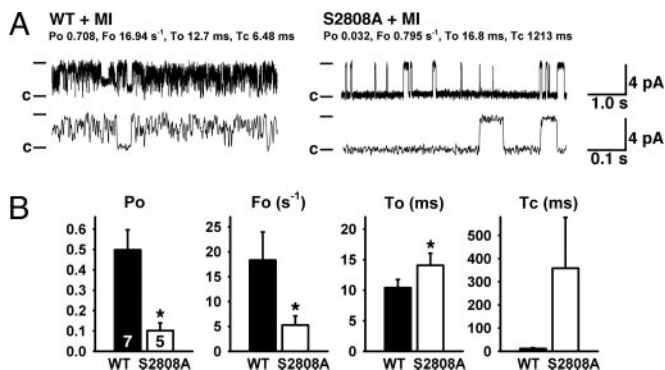
Fig. 5. Normalized RyR2 channel function in RyR2-S2808A mice after MI. (*A*) RyR2 channels isolated from hearts 28 days after MI showed reduced Po in RyR2-S2808A mice compared with WT. Representative single-channel tracings are shown at 150 nM Ca^{2+}. Fo, frequency of channel opening (s^{-1}); To, average open time (ms); and Tc, average closed time (ms); values correspond to the representative tracing shown. Duration upper tracings, 5 s; bottom tracings, 0.5 s. Current amplitude of full openings is 4 pA; c, closed state of channel. (*B*) Bar graphs show mean values for WT (*n* = 7 channels) and RyR2-S2808A (*n* = 5 channels). *, *P* < 0.05.

progressive cardiac dysfunction in mice with ischemia-induced HF. Using genetically altered mice in which Ser-2808 on RyR2 has been replaced by Ala, we showed that Ser-2808 is the only functionally important PKA phosphorylation site in murine and human RyR2 channels. Because previous studies have shown that HF causes chronic PKA hyperphosphorylation of RyR2 leading to altered intracellular Ca^{2+} homeostasis that contributes to decreased cardiac contractility, our findings suggest that selective inhibition of RyR2 PKA hyperphosphorylation and/or its consequences (including calstabin2 depletion from the RyR2 channel complex) may represent a significant therapeutic strategy for the treatment of HF after MI.

Several studies have indicated that Ser-2808 is the only PKA phosphorylation site on RyR2; however, these findings have been challenged. The results from the present study by using a previously undeveloped RyR2-S2808A mouse, clearly indicate a unique and important role for Ser-2808 during physiological RyR2 channel regulation by the SNS *in vivo*. Originally, on the basis of phospho-peptide mapping, PKA was proposed to phosphorylate Ser-2808 on RyR2, in addition to CaMKII (20, 28). We recently identified the actual CaMKII phosphorylation site on RyR2, Ser-2814, which is six residues away from the PKA site (19). Moreover, we used site-directed mutagenesis of GST-fusion proteins (8), mutations in the full-length recombinant RyR2 (19, 21), and immunoblotting by using phospho-epitope-specific antibodies (19, 25, 29) to identify Ser-2808 as the functionally important PKA site on RyR2. In contrast, a recent study by Xiao *et al.* (15) suggested that Ser-2031 on human RyR2 (Ser-2030 on murine RyR2) might constitute an additional PKA phosphorylation site. Using phospho-epitope specific antibodies, Xiao *et al.* (15) found that both Ser-2808 and Ser-2031 are PKA-phosphorylated after exposure of isolated rat cardiomyocytes to high doses of isoproterenol. Our data do not support these findings because the stoichiometry of [^{32}P]-ATP incorporation after PKA phosphorylation was the same for RyR2-WT and RyR2-S2031A channels (Fig. 2*A*). Moreover, i.v. isoproterenol infusion in RyR2-S2808A mice or isoproterenol treatment of isolated RyR2-S2808A cardiomyocytes did not result in measurable PKA phosphorylation of RyR2 (Fig. 1*E*). Thus, the present data indicate that *in vivo*, only one PKA site in RyR2 (Ser-2808) is phosphorylated upon activation of the β-adrenergic signaling pathway. Because the study by Xiao *et al.* (15) was based on the use of recombinant murine RyR2, it is possible that

a sequence difference could account for an additional PKA site that is not present in the native murine RyR2.

Multiple studies have shown that phosphorylation by PKA increases the Po of RyR2 by increasing the sensitivity of RyR2 to Ca^{2+}-induced activation (4, 8, 19, 30, 31). Conversely, some studies reported that RyR2 was not PKA-phosphorylated during stress (16) or that PKA phosphorylation does not increase RyR2 Po (32). Our present study demonstrates that RyR2 is phosphorylated by PKA *in vivo* and agrees with earlier studies showing that RyR2 is PKA-phosphorylated at Ser-2808 during exercise (21) and after isoproterenol infusion. Moreover, single-channel studies in planar lipid bilayers confirmed that PKA phosphorylation increased the Po of both RyR2-WT and RyR2-S2031A channels (Fig. 2*B*). In contrast, PKA phosphorylation did not increase the activity of RyR2-S2808A channels, consistent with a complete functional knockout of the PKA phosphorylation site on RyR2 in the RyR2-S2808A mice.

Biochemical and single-channel studies have shown that PKA phosphorylation of RyR2 dissociates the channel-stabilizing subunit calstabin2 from the channel complex (8, 33). Our present data are consistent with these studies because PKA phosphorylation of RyR2-WT channels decreased calstabin2 binding (Fig. 2*A*) and increased the channel Po. Consistent with previous studies (19), PKA phosphorylation of RyR2-S2808A mutant channels failed to deplete calstabin2 from the channel complex, indicating that PKA phosphorylation of Ser-2808 reduces calstabin2 binding to the channel. On the other hand, mutating Ser-2031 to an Ala did not alter the effects of PKA phosphorylation on calstabin2 binding to RyR2. Thus, at the functional level, the only important PKA site on RyR2 is Ser-2808.

In intact cardiomyocytes, PKA phosphorylation of RyR2 is thought to contribute to enhanced Ca^{2+} transients during β-adrenergic stimulation, resulting in enhanced cardiac contractility (10, 30). Several mechanisms have been proposed for this gain in Ca^{2+}-induced Ca^{2+} release, including increased Ca^{2+} sensitivity of PKA-phosphorylated RyR2 (8), altered luminal modulation of RyR2 (34), increased SR Ca^{2+} load (35, 36), and increased trigger Ca^{2+} release through the L-type Ca^{2+} channel (37). The finding that myocardial contractility is higher in RyR2-S2808A mice after MI supports an important role for PKA phosphorylation of RyR2 in the downstream effects of β-adrenergic signaling. These observations are consistent with recent studies (30) demonstrating that β-adrenergic stimulation results in enhanced, highly localized Ca^{2+} release signals, resulting from PKA phosphorylation of RyR2. This finding is important because it clearly shows that the amplitude of the global cellular Ca^{2+} release, which depends on SR Ca^{2+} load, is not a reliable measure of RyR2 regulation (30). Additionally, Ginsburg and Bers (10) observed a 50% increase in the maximal rate of SR Ca^{2+} release after β-adrenergic stimulation when they compared fractional SR Ca^{2+} release before and after isoproterenol over a broad range of controlled I_{Ca} triggers and SR Ca^{2+} loads. These cellular studies, together with our current findings, provide a better understanding of the mechanisms by which E-C coupling is regulated during β-adrenergic stimulation.

HF is characterized by a chronic hyperadrenergic state, in which elevated levels of circulating catecholamines secondary to chronic SNS activation cause PKA hyperphosphorylation of RyR2 (Fig. 6). Biochemical studies have demonstrated that PKA phosphorylation of RyR2 is associated with decreased binding of the calstabin2 regulatory subunit (8). PKA hyperphosphorylated and calstabin2-depleted channels are prone to aberrant channel openings, causing diastolic SR Ca^{2+} leak and net depletion of the SR Ca^{2+} stores. An important unanswered question, however, was whether PKA hyperphosphorylation of RyR2 contributes to depressed force generation and the progression of HF by this mechanism.
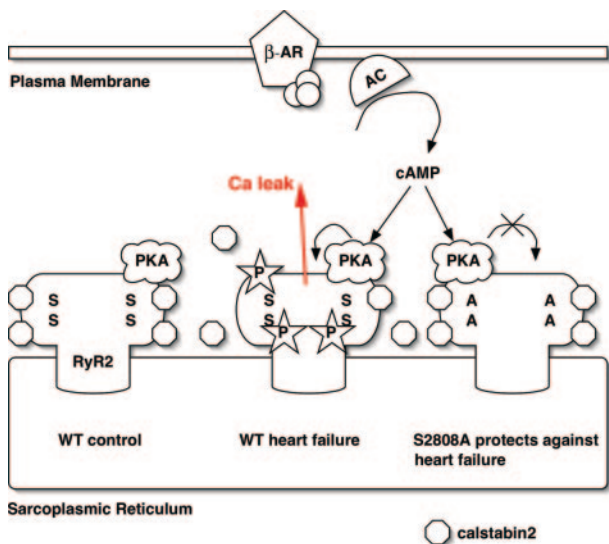
Fig. 6. Proposed model of mechanism by which inhibition of PKA phosphorylation of RyR2 prevents intracellular Ca^{2+} leak in heart failure. (*Left*) The cardiac ryanodine receptor exists in clusters of tetrameric calcium-release channels located on the SR membrane. Each RyR2 monomer contains one PKA phosphorylation site Ser-2808 (S) and binds one PKA enzyme complex (in the cartoon, only one PKA complex is shown per tetrameric channel). (*Middle*) During heart failure, persistent activation of the fight-or-flight stress response causes chronic activation of the β-adrenergic signaling pathway and PKA hyperphosphorylation of RyR2 (stars depict posttranslational modification by PO_4 molecules). Chronic PKA hyperphosphorylation of RyR2 is associated with calstabin2 depletion of the channel complex (symbolized by dissociation of octagons from RyR2). (*Right*) In RyR2-S2808A mice, substitution of Ser-2808 by Ala prevents RyR2 PKA hyperphosphorylation and SR Ca^{2+} leak that has beneficial effects, including reduced maladaptive remodeling after MI.

Our present data suggest that genetic disruption of RyR2 PKA hyperphosphorylation inhibits the progression of cardiac dysfunction in mice after MI. Because RyR2 in the hearts of RyR2-S2808A mice cannot be PKA-phosphorylated, calstabin2 levels in the RyR2 macromolecular complex are not reduced as they are in WT mice during HF, despite significant cardiac remodeling after MI. These findings suggest that PKA hyperphosphorylation is indeed the molecular trigger responsible for reduced calstabin2 levels in the RyR2 channel complex in failing hearts (8, 23, 25, 38).

In agreement with our findings, Bers and colleagues (39) have recently confirmed PKA hyperphosphorylation of RyR2, depletion of calstabin2 from the RyR2 complex, the existence of a diastolic SR Ca^{2+} leak in failing hearts, and the resulting depletion of SR Ca^{2+} predicted by our findings. However, in contrast to our findings showing that the diastolic SR Ca^{2+} leak is mediated by the PKA hyperphosphorylation of RyR2, Bers and colleagues (39) have proposed that it is CaMKII phosphorylation of RyR2 that causes the leak. However, in their experiments, Bers and colleagues (39) did not control for the likely increase in heart rate observed in their rabbit heart failure model, and we previously have reported that the increase in heart rate alone in nonfailing rabbit hearts is sufficient to cause increased CaMKII phosphorylation of RyR2 but without dissociation of calstabin2 (19). Indeed, we have proposed that the increased CaMKII phosphorylation of RyR2 is important for the positive force-frequency relationship observed in healthy hearts but absent in failing hearts (19).

Previous studies by using the 1,4-benzothiazepine JTV519, which increases the binding of calstabin2 to PKA phosphorylated RyR2, revealed similar findings, e.g., improved cardiac function in mice or dogs with heart failure (14, 38). Thus, prevention of

aberrant diastolic intracellular Ca^{2+} release through leaky RyR2 enhances cardiac contractility in mice with ischemic heart failure. Because the mutation RyR2-S2808A is not cardiac-specific, and RyR2 is also expressed in other organs such as the brain, pancreas, and smooth muscle, it is possible that some of the benefits reported in RyR2-S2808A mice after MI may be related to extra-cardiac effects. However, the increase in cardiac contractility is most likely related to the preservation of normal Ca^{2+} homeostasis by virtue of the prevention of diastolic SR Ca^{2+} leak via defective RyR2.

In the face of the well documented down-regulation of the β-adrenergic signaling components in heart failure, PKA hyperphosphorylation of RyR2 is an unexpected finding (8). However, down-regulation of phosphatase levels in the RyR2 complex in HF provides one possible mechanism for chronically increased RyR2 PKA phosphorylation in HF (8). In addition, recent data from our laboratory indicate that in human and animal models of HF, local cAMP levels in the RyR2 microdomain are increased because of reduced PDE4D3 activity in the RyR2 channel complex (11). Indeed, we have observed that haploin-sufficient $PDE4D^{+/-}$ mice exhibit enhanced cardiac dysfunction after MI. Interestingly, $PDE4D^{+/-}$ mice crossed with the RyR2-S2808A mice described in the present study were relatively protected against the development of HF after MI. Thus, the RyR2-S2808A mutation protects against the development of HF that results from PDE4D deficiency.

In addition to causing contractile defects, diastolic SR Ca^{2+} leak due to PKA hyperphosphorylation of RyR2 can also provide triggers for fatal cardiac arrhythmias. Inherited missense mutations in RyR2 result in a gain-of-function defect that causes a diastolic SR Ca^{2+} leak during β-adrenergic stimulation (21). Because these mutant RyR2 channels have a decreased calstabin2 binding affinity, they are more likely to open aberrantly during diastole (21, 40). Accordingly, calstabin2-deficient mice develop delayed after-depolarizations and ventricular arrhythmias during exercise or stress (21). Similarly, *PDE4D*-deficient mice, or WT mice treated with the PDE4 inhibitor rolipram, exhibit PKA-hyperphosphorylated RyR2 due to significantly decreased cAMP hydrolysis and are more susceptible to stress-induced ventricular arrhythmias (11). Interestingly, RyR2-S2808A mice treated with the PDE4 inhibitor rolipram were protected against exercise-induced arrhythmias (11), providing further evidence that PKA hyperphosphorylation of RyR2 plays an important role in triggering cardiac arrhythmias and sudden death.

The present study demonstrates that a single amino acid, Ser-2808, in the RyR2 channel plays a major role in determining the progression of cardiac dysfunction after MI (Fig. 6). The finding that the substitution of an Ala for RyR2 Ser[2808] can protect against post-MI HF is surprising because HF is a complex multifactorial disorder and there currently is no treatment that effectively prevents the progressive cardiac dysfunctions in many patients after MI. The importance of RyR2 Ser[2808] is perhaps linked to its critical role as a mediator of the fight-or-flight survival stress response (Fig. 6). The fight-or-flight response is likely one of the more primitive survival stress responses in many organisms including humans. Indeed many of the sequences in RyR2 involved in mediating this response have been conserved from *Caenorhabditis elegans* to humans (12). The role of PKA phosphorylation of RyR2 at Ser[2808] may have been to facilitate rapid increases in activity, such as going from rest to full sprint, which is required to escape predators. This role would explain why this system has been preserved through evolution and why it is no longer required for survival. Indeed, as longevity increases in humans, the formerly protective response that enabled our ancestors to escape predators is now turned against us and appears to contribute significantly to the progression of HF, a leading cause of mortality.

Our data reveal the key importance of RyR2-Ser-2808 and provide strong support for therapeutic approaches aimed at counteracting the functional effects of maladaptive chronic PKA hyperphosphorylation of this residue in the RyR2 channel (Fig. 6). One possible therapeutic approach would be to prevent PKA phosphorylation of RyR2, indeed this effect is what β-adrenergic receptor blockers achieve (22, 24, 25), and they have been shown to increase survival in HF patients. However, β-adrenergic receptor blockers have unacceptable side effects that often limit their use by patients (including lethargy, depression, impotence, hypotension, and bradycardia). A more targeted approach would be to prevent the consequences of PKA phosphorylation of RyR2, namely dissociation of calstabin2 from the channel, which results in the leaky channel phenotype. We have shown that compounds in the 1,4-benzothiazepine class, known as "calcium channel stabilizers" increase the binding affinity of calstabin2 to PKA phosphorylated RyR2, prevent the channel leak, and improve cardiac function and prevent sudden cardiac death in relevant animal models (14, 27). The present study provides evidence for the importance of PKA phosphorylation of RyR2 as a therapeutic target for HF and sudden cardiac death.

Materials and Methods

Generation of RyR2-S2808A Mice. Murine genomic RyR2 clones were isolated from a 129/SvEvTacfBR λ-phage library (Stratagene, La Jolla, CA) (Fig. 1A). A 5.4-kb EcoRI fragment containing exons 53 to 55 was isolated by using a 250-bp [32P]-labeled RyR2 cDNA probe encoding Ser-2808 and flanking sequences and subcloned into the EcoRI site of pBluescriptSK (Fig. 1B). The 3′ targeting arm consisting of the 2,463 bp upstream of the EcoRI site was obtained by PCR of murine genomic DNA. After adding SalI sites to both ends of this 2.4-kb fragment, it was cloned into the SalI site of the pACN vector, which contains genes for neomycin resistance, Cre recombinase and a testes-specific promoter (tACE), flanked by loxP sites (41) (Fig. 1B). After mutagenesis of Ser-2808 to Ala by using a Chameleon Mutagenesis Kit (Stratagene), the EcoRI fragment was cloned into the pACN vector (Fig. 1C). The tACE promoter initiates expression of Cre recombinase only during spermatogenesis, resulting in excision of the ACN cassette (Fig. 1D).

The KpnI linearized targeting vector was electroporated into MM13 mouse embryonic stem (ES) cells. Targeted ES cells were screened by Southern blot analysis by using both 5′ and 3′ external probes to confirm homologous recombination. Subsequently, an 1,130-bp fragment containing the mutated RyR2 exon was amplified by PCR and then cut with FspI to screen for the S2808A mutation. Successfully targeted ES cells were injected into C57Bl6 blastocysts, and founders were backcrossed to C57Bl6 mice. Germline offspring were identified by brown coat color and further verified by Southern blot analyses. Heterozygous males and females were intercrossed to obtain homozygous RyR2-S2808A offspring.

Surgical and Animal Procedures. RyR2-S2808A mice and age-matched WT littermates were maintained and studied according to protocols approved by the Institutional Animal Care and Use Committee of Columbia University. Mice were randomized to undergo either MI or a sham procedure. Ligation of the left anterior descending artery was performed as described in ref. 14. Four weeks after MI, mice were anesthetized with 1.5% isoflurane in O_2 and placed on a heating pad (37°C). Cardiac function was assessed by echocardiography with a Hewlett Packard Sonos 5500 ultrasound with a 12-MHz transducer applied to the chest wall. Cardiac ventricular dimensions were measured in M mode. In addition, cardiac catheterization was used to assess contractility with a 1.4F high-fidelity micromanometer catheter (Millar Instruments), advanced via the right carotid artery into the left ventricle (14). The IOX data acquisition system was used to analyze pressure-volume relationships (Emka Technologies, Falls Church, VA).

Immunocytochemistry. Cardiac myocytes were isolated from adult WT and RyR2-S2808A mice by using established methods (42). Murine hearts were removed, the aorta cannulated by using a Langendorff perfusion system and retrogradely perfused with a Ca^{2+}-free solution for <5 min. For enzymatic digestion, collagenase type 2 (0.5 mg/ml, Worthington) was added to the perfusion solution for 20 min. After digestion, ventricles were cut into small pieces, gently agitated, and $[Ca^{2+}]$ was gradually increased to a final concentration of 1 mM.

Isolated cardiomyocytes were transferred into normal Tyrode solution and exposed to isoproterenol (1.0 μM) for 10 min at room temperature, as indicated. Cells were fixed by incubation in 100% ethanol for 30 min at -20°C. After washing four times for 20 min by using wash/block buffer (PBS supplemented with 5.0% normal goat serum and 3.0% BSA), myocytes were incubated in primary antibody (1:400) overnight at 4°C. After washing four times in wash/block buffer, myocytes were incubated with secondary antibody (goat anti-rabbit, Alexa 488, Molecular Probes). After four washes in wash/block buffer, cells were imbedded in SlowFade Gold Antifade reagent. Cardiomyocytes were imaged on a Zeiss LSM 510 inverted laser-scanning microscope by using a ×63 oil immersion objective.

Histological Analysis. After hemodynamic analyses, hearts were arrested in diastole and perfused antegradely at physiological pressures with PBS containing 0.5 mM KCl. Heart tissue was fixed in 3.7% buffered formaldehyde, cut transversely through the maximal diameter of the infarcted area, and embedded in paraffin. Sections (4 μm) were stained with hematoxylin and eosin, and infarct size was calculated as total infarct circumference divided by total left ventricle circumference.

RyR2 Phosphorylation. RyR2 was immunoprecipitated by incubating 500 μg of mouse ventricular homogenate with anti-RyR antibody in 0.5 ml of a modified radioimmunoprecipitation assay buffer [RIPA; 50 mM Tris·HCl buffer (pH 7.4)/0.9% NaCl/5.0 mM NaF/1.0 mM Na_3VO_4/0.5% Triton X-100/protease inhibitors] as described in ref. 44. After incubation with protein A-Sepharose beads for 1 h, samples were transferred into 10 μl of 1.5× phosphorylation buffer (8 mM $MgCl_2$/10 mM EGTA/50 mM Tris/Pipes, pH 6.8) containing either alkaline phosphatase (AP, 1:100, New England Biolabs) or PKA catalytic subunit (Sigma, St. Louis, MO), with or without inhibitor PKI_{5-24} (500 nM, Calbiochem, San Diego). The stoichiometry of RyR2 PKA phosphorylation was determined by using [32P]-ATP standards. The [32P]/RyR2 ratio was calculated by dividing [32P]-phosphorylation of RyR2 by the amount of high-affinity [3H]-ryanodine binding, as described in ref. 43.

Back phosphorylation of immunoprecipitated RyR2 was initiated with 33 μM Mg-ATP containing 10% [γ-32P]-ATP (PerkinElmerLife Sciences, Boston) and terminated after 8 min at room temperature with 5 μl of stop solution (4% SDS/0.25 M DTT). Samples were heated to 95°C, size-fractionated on 6% SDS/PAGE, and RyR2 radioactivity was quantified by using a PhosphorImager and IMAGEQUANT software (Amersham Pharmacia Biosciences, Piscataway, NJ). PKA phosphorylation of RyR2 correlates with the inverse of the PKA-dependent [γ-32P]-ATP signal.

Western Blot Analysis. Western blot analysis was performed by using primary antibodies against calstabin2 (FKBP12.6, 1:1,000), RyR2 (5029; 1:3,000), RyR2-pSer[2808] (1:5,000), RyR2-pSer[2814] (1:2,000), phospholamban (PLB, Affinity BioReagents, 1:5,000), PLB-Ser-16 (Research Diagnostics, 1:5,000), PLB-Thr-17 (Badrilla, 1:5,000), and SERCA2a (1:2,000), for 1 h at room

temperature. Band densities were quantified by using QUANTITY ONE software (Bio-Rad, Hercules, CA).

Generation and Expression of RyR2 Phosphorylation Site Mutants. RyR2-S2808A and RyR2-S2808D were generated in the human RyR2 cDNA as described in ref. 19. RyR2-S2031A and RyR2-S2031D were generated by using the QuikChange site-directed mutagenesis kit (Stratagene) in a pBlueScript⁻ subcloning vector containing the ClaI-KpnI RyR2-fragment (nucleotides 2472–7678) with the following primers: (S2031A), 5′-GAGGGCGTCT-GCTA*GCG*CTGGTAGAAAAGGTGAC; and (S2031D), 5′-GAGGGCGTCTGCTA*GAC*CTGGTAGAAAAGGTGAC. Silent NheI (S2031A) or SexAI (S2031D) restriction sites were introduced to facilitate screening of mutant clones. Fragments containing the mutation were cloned into pCMV5-RyR2 by using BstEII and Acc65I restriction enzymes. Recombinant WT and mutant RyR2 channels were coexpressed in HEK293 cells together with calstabin2 (FKBP12.6), as described in ref. 19.

Single-Channel Recordings. Vesicles containing RyR2 were incorporated into planar lipid bilayers in 100-μm holes in polystyrene cups separating two chambers. The trans chamber (1.0 ml) representing the intra-SR compartment was connected to the head stage input of a bilayer voltage-clamp amplifier (Warner Instruments, Hamden, CT). The cis chamber (1.0 ml) representing the cytoplasmic compartment was held at virtual ground. Chamber solutions were as follows: trans 250 mM Hepes and 53 mM Ca(OH)$_2$, pH 7.35; cis 250 mM Hepes, 125 mM Tris, 1.0 mM EGTA, and 0.5 mM CaCl$_2$, pH 7.35. At the conclusion of each experiment, ryanodine (5 μM) or ruthenium red (20 μM) were applied to confirm RyR2 channel identity.

Statistical Analysis. Statistical analyses between the experimental groups were performed by using a Student's t test or one-way ANOVA when comparing multiple groups. Data were reported as mean $\pm$ SEM. Values of $P \leq 0.05$ were considered significant.

1. Moss, A. J. (2005) *Ann. Noninvasive Electrocardiol.* **10,** 279–280.
2. Wehrens, X. H. & Marks, A. R. (2004) *Ann. Med.* **36,** Suppl. 1, 70–80.
3. Lakatta, E. G. (2004) *Cell Calcium* **35,** 629–642.
4. Wehrens, X. H. T., Lehnart, S. E. & Marks, A. R. (2005) *Annu. Rev. Physiol.* **67,** 69–98.
5. Song, L. S., Wang, S. Q., Xiao, R. P., Spurgeon, H., Lakatta, E. G. & Cheng, H. (2001) *Circ. Res.* **88,** 794–801.
6. Viatchenko-Karpinski, S. & Gyorke, S. (2001) *J. Physiol.* **533,** 837–848.
7. Gomez, A. M., Valdivia, H. H., Cheng, H., Lederer, M. R., Santana, L. F., Cannell, M. B., McCune, S. A., Altschuld, R. A. & Lederer, W. J. (1997) *Science* **276,** 800–806.
8. Marx, S. O., Reiken, S., Hisamatsu, Y., Jayaraman, T., Burkhoff, D., Rosemblit, N. & Marks, A. R. (2000) *Cell* **101,** 365–376.
9. Kiss, E., Edes, I., Sato, Y., Luo, W., Liggett, S. B. & Kranias, E. G. (1997) *Am. J. Physiol.* **272,** H785–H790.
10. Ginsburg, K. S. & Bers, D. M. (2004) *J. Physiol.* **556,** 463–480.
11. Lehnart, S. E., Wehrens, X. H. T., Reiken, S. R., Warrier, S., Belevych, A. E., Harvey, R. D., Richter, W., Jin, S. L. C., Conti, M. & Marks, A. R. (2005) *Cell* **123,** 25–35.
12. Marx, S. O., Reiken, S., Hisamatsu, Y., Gaburjakova, M., Gaburjakova, J., Yang, Y. M., Rosemblit, N. & Marks, A. R. (2001) *J. Cell Biol.* **153,** 699–708.
13. Marks, A. R. (2000) *Circ. Res.* **87,** 8–11.
14. Wehrens, X. H., Lehnart, S. E., Reiken, S., van der Nagel, R., Morales, R., Sun, J., Cheng, Z., Deng, S. X., de Windt, L. J., Landry, D. W. & Marks, A. R. (2005) *Proc. Natl. Acad. Sci. USA* **102,** 9607–9612.
15. Xiao, B., Jiang, M. T., Zhao, M., Yang, D., Sutherland, C., Lai, F. A., Walsh, M. P., Warltier, D. C., Cheng, H. & Chen, S. R. (2005) *Circ. Res.* **96,** 847–855.
16. Jiang, M. T., Lokuta, A. J., Farrell, E. F., Wolff, M. R., Haworth, R. A. & Valdivia, H. H. (2002) *Circ. Res.* **91,** 1015–1022.
17. Hasenfuss, G., Mulieri, L. A., Leavitt, B. J., Allen, P. D., Holubarsch, C., Just, H. & Alpert, N. R. (1992) *Basic Res. Cardiol.* **87,** Suppl. 1, 107–116.
18. Pieske, B., Kretschmann, B., Meyer, M., Holubarsch, C., Weirich, J., Posival, H., Minami, K., Just, H. & Hasenfuss, G. (1995) *Circulation* **92,** 1169–1178.
19. Wehrens, X. H., Lehnart, S. E., Reiken, S. R. & Marks, A. R. (2004) *Circ. Res.* **94,** e61–e70.
20. Witcher, D. R., Kovacs, R. J., Schulman, H., Cefali, D. C. & Jones, L. R. (1991) *J. Biol. Chem.* **266,** 11144–11152.
21. Wehrens, X. H., Lehnart, S. E., Huang, F., Vest, J. A., Reiken, S. R., Mohler, P. J., Sun, J., Guatimosim, S., Song, L. S., Rosemblit, N., *et al.* (2003) *Cell* **113,** 829–840.
22. Reiken, S., Gaburjakova, M., Gaburjakova, J., He Kl, K. L., Prieto, A., Becker, E., Yi Gh, G. H., Wang, J., Burkhoff, D. & Marks, A. R. (2001) *Circulation* **104,** 2843–2848.
23. Yano, M., Ono, K., Ohkusa, T., Suetsugu, M., Kohno, M., Hisaoka, T., Kobayashi, S., Hisamatsu, Y., Yamamoto, T., Noguchi, N., *et al.* (2000) *Circulation* **102,** 2131–2136.
24. Doi, M., Yano, M., Kobayashi, S., Kohno, M., Tokuhisa, T., Okuda, S., Suetsugu, M., Hisamatsu, Y., Ohkusa, T. & Matsuzaki, M. (2002) *Circulation* **105,** 1374–1379.
25. Reiken, S., Wehrens, X. H., Vest, J. A., Barbone, A., Klotz, S., Mancini, D., Burkhoff, D. & Marks, A. R. (2003) *Circulation* **107,** 2459–2466.
26. Luo, W., Chu, G., Sato, Y., Zhou, Z., Kadambi, V. J. & Kranias, E. G. (1998) *J. Biol. Chem.* **273,** 4734–4739.
27. Wehrens, X. H., Lehnart, S. E., Reiken, S. R., Deng, S. X., Vest, J. A., Cervantes, D., Coromilas, J., Landry, D. W. & Marks, A. R. (2004) *Science* **304,** 292–296.
28. Takasago, T., Imagawa, T., Furukawa, K., Ogurusu, T. & Shigekawa, M. (1991) *J. Biochem. (Tokyo)* **109,** 163–170.
29. Rodriguez, P., Bhogal, M. S. & Colyer, J. (2003) *J. Biol. Chem.* **278,** 38593–38600.
30. Lindegger, N. & Niggli, E. (2005) *J. Physiol.* **565,** 801–813.
31. Takasago, T., Imagawa, T. & Shigekawa, M. (1989) *J. Biochem. (Tokyo)* **106,** 872–877.
32. Li, Y., Kranias, E. G., Mignery, G. A. & Bers, D. M. (2002) *Circ. Res.* **90,** 309–316.
33. Kaftan, E., Marks, A. R. & Ehrlich, B. E. (1996) *Circ. Res.* **78,** 990–997.
34. Gyorke, I. & Gyorke, S. (1998) *Biophys. J.* **75,** 2801–2810.
35. Bassani, J. W., Yuan, W. & Bers, D. M. (1995) *Am. J. Phys.* **268,** C1313–C1319.
36. Terentyev, D., Viatchenko-Karpinski, S., Gyorke, I., Volpe, P., Williams, S. C. & Gyorke, S. (2003) *Proc. Natl. Acad. Sci. USA* **100,** 11759–11764.
37. Reuter, H., Zobel, C., Brixius, K., Bolck, B. & Schwinger, R. H. (1999) *Basic Res. Cardiol.* **94,** 159–170.
38. Yano, M., Kobayashi, S., Kohno, M., Doi, M., Tokuhisa, T., Okuda, S., Suetsugu, M., Hisaoka, T., Obayashi, M., Ohkusa, T. & Matsuzaki, M. (2003) *Circulation* **107,** 477–484.
39. Ai, X., Curran, J. W., Shannon, T. R., Bers, D. M. & Pogwizd, S. M. (2005) *Circ. Res.* **97,** 1314–1322.
40. Lehnart, S. E., Wehrens, X. H. T., Laitinen, P. J., Reiken, S. R., Deng, S. X., Chen, Z., Landry, D. W., Kontula, K., Swan, H. & Marks, A. R. (2004) *Circulation* **109,** r113–r119.
41. Bunting, B., Bernstein, K. E., Greer, J. M., Capecchi, M. R. & Thomas, K. R. (1999) *Genes Dev.* **13,** 1524–1528.
42. DelPrincipe, F., Egger, M. & Niggli, E. (1999) *Nat. Cell Biol.* **1,** 323–329.
43. Reiken, S., Gaburjakova, M., Guatimosim, S., Gomez, A. M., D'Armiento, J., Burkhoff, D., Wang, J., Vassort, G., Lederer, W. J. & Marks, A. R. (2003) *J. Biol. Chem.* **278,** 444–453.